

Design and Performance Analysis of a New Class of Rate Compatible Serial Concatenated Convolutional Codes

Alexandre Graell i Amat, *Member, IEEE*, Guido Montorsi, *Senior Member, IEEE*,
and Francesca Vatta, *Member, IEEE*

Abstract

In this paper, we provide a performance analysis of a new class of serial concatenated convolutional codes (SCCC) where the inner encoder can be punctured beyond the unitary rate. The puncturing of the inner encoder is not limited to inner coded bits, but extended to systematic bits. Moreover, it is split into two different puncturings, in correspondence with inner code systematic bits and parity bits. We derive the analytical upper bounds to the error probability of this particular code structure and address suitable design guidelines for the inner code puncturing patterns. We show that the percentile of systematic and parity bits to be deleted strongly depends on the SNR region of interest. In particular, to lower the error floor it is advantageous to put more puncturing on inner systematic bits. Furthermore, we show that puncturing of inner systematic bits should be interleaver dependent. Based on these considerations, we derive design guidelines to obtain well-performing rate-compatible SCCC families. Throughout the paper, the performance of the proposed codes are compared with analytical bounds, and with the performance of PCCC and SCCC proposed in the literature.

Index Terms

This work has been partially funded by MEC under JdC contract. The material in this paper was presented in part at the IEEE International Symposium on Information Theory, Adelaide, Australia, September 2005.

A. Graell i Amat is with the Department of Electronics, Politecnico di Torino, 10129 Torino, Italy, and with the Department of Technology, Universitat Pompeu Fabra, 30100 Barcelona, Spain. (e-mail: alexandre.graell@polito.it).

G. Montorsi is with the Department of Electronics, Politecnico di Torino, 10129 Torino, Italy. (e-mail: montorsi@polito.it).

F. Vatta is with DEEI, Università di Trieste, 34127 Trieste, Italy. (e-mail: vatta@univ.trieste.it).

Serial concatenated convolutional codes, iterative decoding, rate-compatible codes, Turbo codes, performance bounds.

I. INTRODUCTION

Rate-compatible codes were introduced for the first time in [1], where the concept of punctured codes was extended to the generation of a family of rate-compatible punctured convolutional (RCPC) codes. The rate-compatibility restriction requires that the rates are organized in a hierarchy, where all code bits of a high rate punctured code are used by all the lower rate codes. Based on RCPC codes, Hagenauer proposed an ARQ strategy which provides a flexible way to accommodate code rate to the error protection requirements, or varying channel conditions. Furthermore, rate-compatible codes can be used to provide unequal error protection (UEP). The concept of rate-compatible codes has then been extended to parallel and serial concatenated convolutional codes [2–4].

Recently, a new class of hybrid serial concatenated codes was proposed in [5] with bit error performance between that of PCCC and SCCC. A similar concept has been presented in [6] to obtain well performing rate-compatible SCCC families. To obtain rate-compatible SCCC, the puncturing is limited to inner coded bits. However, in contrast to standard SCCC, codes in [6] are obtained puncturing both inner parity bits and systematic bits, thereby obtaining rates beyond the outer code rate. With this assumption, puncturing is split into two puncturing patterns, for both systematic and parity bits. This particular code structure offers very good performance over a range of rates, including very high ones, and performs better than standard SCCC.

The optimization problem of this particular code structure consists in optimizing these two puncturing patterns and finding the optimal proportion of inner code systematic and parity bits to be punctured to obtain a given rate. Some design criteria to obtain good rate-compatible SCCC families are discussed in [6]. However, the considerations in [6] are limited to *heuristic* design guidelines, with no theoretical analysis support. Thus, a deeper and more formal insight on the performance of this new class of SCCC is required, in order to provide suitable design guidelines aimed at the code optimization.

In this paper, we provide a performance analysis of this new class of concatenated codes. By properly redrawing the SCCC as a parallel concatenation of two codes, we derive the analytical upper bounds to the error probability using the concept of *uniform interleaver*. We then propose

suitable design criteria for the inner code puncturing patterns, and to optimize the proportion of inner systematic and parity bits to be deleted. We show that the optimal percentage of bits to be punctured depends on the SNR region of interest. In particular, it is shown that to improve the performance in the error floor region, it is advantageous to increase the proportion of surviving inner code parity bits, as far as a sufficient number systematic bits is kept. Moreover, the optimal puncturing of the inner code systematic bits depends on the outer encoder and, thus, it must be interleaver dependent. Finally, based on these considerations, we address design guidelines to obtain well-performing SCCC families.

The paper is organized as follows. In the next section, we describe the new class of concatenated codes addressed in the paper. In Section III, the upper bounds to the residual bit error probability and frame error probability of this new class of codes are derived and design criteria are outlined. Design guidelines to obtain well-performing SCCC families are discussed in Section IV. In Section V, simulation results are compared with the analytical upper bounds. Finally, in Section VI we draw some conclusions.

II. A NEW CLASS OF SERIAL CONCATENATED CONVOLUTIONAL CODES

Throughout the paper we shall refer to the encoder scheme shown in Fig. 1.

We consider the serial concatenation of two systematic recursive convolutional encoders. To obtain high rates both encoders are punctured. However, in contrast to standard SCCC where high rates are obtained by concatenating an extensively punctured outer encoder with an inner encoder of rate $R_c^i \leq 1$ such that the rate of the SCCC, R_{SCCC} , is at most equal to the rate of the outer encoder ($R_{\text{SCCC}} \leq R_c^o$), the inner encoder in Fig. 1 can be punctured beyond the unitary rate, i.e., the overall code rate R_{SCCC} can be greater than the outer code rate R_c^o . Moreover, as made evident in the figure, puncturing is not directly applied to the inner code sequence but split into two different puncturings, in correspondence to inner code systematic bits and inner code parity bits (P_i^s and P_i^p , respectively). Assuming an inner mother code of rate $1/n$, the rate of the resulting SCCC is given by

$$R_{\text{SCCC}} = R_c^{o'} R_c^i = R_c^{o'} \frac{1}{\rho_s + (n-1)\rho_p} \quad (1)$$

where $R_c^{o'}$ is the outer code rate after applying the fixed puncturing pattern P_o , and ρ_s (ρ_p) is the systematic permeability (parity permeability) rate, defined as the proportion of inner code

systematic bits (parity bits) which are not punctured. Given a certain desired R_{SCCC} , ρ_s and ρ_p are related by

$$\rho_s = \frac{R_c^{o'}}{R_{\text{SCCC}}} - (n - 1)\rho_p. \quad (2)$$

This particular code structure offers superior performance to that of standard SCCE, especially for high-rates. Notice that for high rates, the exhaustive puncturing of the outer code leads to a poor code in terms of free distance, thus leading to a higher error floor. On the contrary, the code structure discussed here, keeps the interleaver gain for low rates also in the case of very high rates, since the heavy puncturing is moved to the inner encoder. Moreover it is well suited for rate-compatible schemes.

It is clear that the performance of the overall SCCE code depends on puncturing patterns P_o , P_i^s and P_i^p , and, subsequently, on the permeability rates ρ_s and ρ_p , which should be properly optimized. In [6], some *heuristic* design guidelines were given to select ρ_s and ρ_p , leading to well-performing families of rate-compatible SCCEs. However, the work in [6] lacks in providing formal analysis to clarify the behavior of this code structure and to provide a unique framework to properly select ρ_s and ρ_p . The aim of this paper is to address design guidelines to clarify some relevant aspects of this new code structure, and to provide the clues for the code optimization.

The design of concatenated codes with interleavers involves the choice of the interleaver and the constituent encoders. The joint optimization, however, seems to lead to prohibitive complexity problems. In [7] Benedetto and Montorsi proposed a method to evaluate the error probability of parallel concatenated convolutional codes (PCCC) independently from the interleaver used. The method consists in a decoupled design, in which one first designs the constituent encoders, and then tailors the interleaver on their characteristics. To achieve this goal, the notion of *uniform interleaver* was introduced in [7]; the actual interleaver is replaced with the *average* interleaver¹. The use of the uniform interleaver drastically simplifies the performance evaluation of Turbo Codes. Following this approach, the best constituent encoders for serial code construction are found in [8], where the analysis in [7] was extended to SCCEs, giving design criteria for constituent encoders.

In the next section, we gain some analytical insight into the code structure of Fig. 1 to address design guidelines to properly select ρ_s , P_i^s and ρ_p , P_i^p . To this purpose, we derive the analytical

¹This average interleaver is actually the weighted set of all interleavers.

upper bounds to the bit and frame error probability, following the concept of uniform interleaver used in [7] and [8] for PCCC and SCCC. However, we do not treat the code structure of Fig. 1 as a standard SCCC, so we cannot directly apply the considerations in [8]. Indeed, the treatment in [8] would consider the inner encoder (with its puncturing) as a unique *entity*, therefore diluting the contribution of the inner code systematic bits and parity bits to the bound. Instead, our idea is to decouple the contribution of the inner systematic bits and inner parity bits to the error probability bound to better identify how to choose ρ_s, P_i^s and ρ_p, P_i^p . In fact, we shall show that to obtain good SCCC codes in the form of Fig. 1, the selection of the inner code puncturing directly depends on the outer code, which has a crucial effect on performance. This dependence cannot be taken into account by the upper bounds derived in [8] for SCCC.

III. ANALYTICAL UPPER BOUNDS TO THE ERROR PROBABILITY

Following the derivations in [7] and [8] for PCCC and SCCC, in this section we derive the union bound of the bit error probability for the code construction of Fig. 1.

Recalling [8], the bit error probability of a SCCC can be upper bounded through

$$\begin{aligned}
 P_b(e) &< \sum_{w=w_m^o}^{NR_c'} \frac{w}{NR_c'} A^{C_s}(w, H) \Bigg|_{H=e^{-\frac{R_{\text{SCCC}} E_b}{N_0}}} \\
 &= \sum_{h=h_m}^{N/R_c^i} \sum_{w=w_m^o}^{NR_c'} \frac{w}{NR_c'} A_{w,h}^{C_s} e^{-\frac{h R_{\text{SCCC}} E_b}{N_0}}
 \end{aligned} \tag{3}$$

where w_m^o is the minimum weight of an input sequence generating an error event of the outer code, N is the interleaver length, and h_m is the minimum weight of the codewords of the SCCC, C_s , of rate R_{SCCC} . $A^{C_s}(w, H)$ is the *Conditional Weight Enumerating Function* (CWEF) of the overall SCCC code. For a generic serially concatenated code, consisting of the serial concatenation of an outer code C_o with an inner code C_i through an interleaver, the CWEF of the overall SCCC code $A_{w,h}^{C_s}$ can be calculated replacing the actual interleaver with the uniform interleaver and exploiting its properties. The uniform interleaver transforms a codeword of weight l at the output of the outer encoder into all distinct $\binom{N}{l}$ permutations. As a consequence, each codeword of the outer code C_o of weight l , through the action of the uniform interleaver, enters the inner encoder generating $\binom{N}{l}$ codewords of the inner code C_i . The CWEF of the overall SCCC code can then be evaluated from the knowledge of the CWEFs of the outer and inner

codes; the coefficients $A_{w,h}^{C_s}$ are given by

$$A_{w,h}^{C_s} = \sum_{l=0}^N \frac{A_{w,l}^{C_o} \times A_{l,h}^{C_i}}{\binom{N}{l}} \quad (4)$$

where $A_{w,l}^{C_o}$ and $A_{l,h}^{C_i}$ are the coefficients of the CWEFs of the outer and inner codes, respectively.

This is basically the same result obtained in [8]. However, and this is the key novelty of our analysis, to evaluate the performance of the code structure of Fig. 1, instead of proceeding as in [8] using (4), it is more suitable to refer to Fig. 2, which properly redraws the encoder of Fig. 1, for the derivation of the upper bound. Fig. 2 allows us to decouple the contributions of the inner code puncturings P_i^s and P_i^p to the error probability bound. Call C_o'' the code obtained from the puncturing of the outer code C_o through P_o and P' , with $P' = \Pi^{-1}[P_i^s]$, i.e., the de-interleaved version of P_i^s , C_o' the code obtained from the puncturing of the outer code C_o through P_o , and C_i' the inner encoder C_i generating only parity bits punctured through P_i^p , which is fed with an interleaved version of codewords generated by C_o'' ². Now, the serial concatenated code structure under consideration can be interpreted as the parallel concatenation of the code C_o'' and C_i' . Therefore, the SCCC codeword weight h can be split into two contributions j and m , corresponding to the output weights of the codewords generated by encoder C_o'' and by encoder C_i' , respectively, such that $h = j + m$. With reference to Fig. 2, equation (4) can then be rewritten as

$$A_{w,h}^{C_s} = A_{w,j+m}^{C_s} = \sum_{l=d_f^{o'}}^N \sum_{j=d_f^{o''}}^{N/R_c^{o''}} \frac{A_{w,l,j}^{C_o''} \times A_{l,m}^{C_i'}}{\binom{N}{l}} \Bigg|_{j+m=h} \quad (5)$$

where $d_f^{o'}$ is the free distance of the code C_o' and $d_f^{o''}$ is the free distance of the code C_o'' . In (5), $R_c^{o''}$ is the rate of the code C_o'' , $A_{w,l,j}^{C_o''}$ indicates the number of codewords of C_o'' of weight j associated with a codeword of C_o' of weight l generated from an information word of weight w ,

²Notice that, in abuse of notation, we have maintained the terminology *outer encoder* and *inner encoder* in Fig. 2 though they do not strictly act as outer and inner encoders. However, we believe that this notation reflects better the correspondence with Fig. 1.

and $A_{l,m}^{C'_i}$ indicates the number of codewords of C'_i of weight m associated with a codeword of C'_o of weight l .

$A_{w,l,j}^{C''_o}$ and $A_{l,m}^{C'_i}$ can be expressed as

$$\begin{aligned} A_{w,l,j}^{C''_o} &\leq \sum_{n^{o''}=1}^{n_M^{o''}} \binom{N/p}{n^{o''}} A_{w,l,j,n^{o''}}^{o''} \\ A_{l,m}^{C'_i} &\leq \sum_{n^{i'}=1}^{n_M^{i'}} \binom{N/p}{n^{i'}} A_{l,m,n^{i'}}^{i'} \end{aligned} \quad (6)$$

where the coefficient $A_{w,l,j,n^{o''}}^{o''}$ represents the number of code C''_o sequences of weight j , associated with a codeword of C'_o of weight l generated from an information word of weight w , and number of concatenated error events $n^{o''}$. In (6), $n_M^{o''}$ is the largest number of error events concatenated in a codeword of the code C''_o of output weight j associated with a codeword of C'_o of weight l and an information word of weight w : $n_M^{o''}$ is a function of w , l and j that depends on the encoder. Also in (6), the coefficient $A_{l,m,n^{i'}}^{i'}$ represents the number of code C'_i sequences of weight m , input weight l , and number of concatenated error events $n^{i'}$. As for $n_M^{o''}$, $n_M^{i'}$ is the largest number of error events concatenated in a codeword of the code C'_i of output weight m generated from an information word of weight l .

Substituting (6) in (5), the value of the coefficients $A_{w,j+m}^{C_s}$ is upper bounded as

$$\begin{aligned} A_{w,j+m}^{C_s} &\leq \sum_{l=d_f^{o'}}^N \sum_{j=d_f^{o''}}^{N/R_c^{o''}} \sum_{n^{o''}=1}^{n_M^{o''}} \sum_{n^{i'}=1}^{n_M^{i'}} \frac{\binom{N/p}{n^{o''}} \binom{N/p}{n^{i'}}}{\binom{N}{l}} \cdot A_{w,l,j,n^{o''}}^{o''} A_{l,m,n^{i'}}^{i'} \\ &\leq \sum_{l=d_f^{o'}}^N \sum_{j=d_f^{o''}}^{N/R_c^{o''}} \sum_{n^{o''}=1}^{n_M^{o''}} \sum_{n^{i'}=1}^{n_M^{i'}} \frac{N^{n^{o''}+n^{i'}-l} l!}{p^{n^{o''}+n^{i'}} n^{o''}! n^{i'}!} \cdot A_{w,l,j,n^{o''}}^{o''} A_{l,m,n^{i'}}^{i'} \end{aligned} \quad (7)$$

Finally, substituting (7) into (3), we obtain the upper bound for the bit error probability,

$$\begin{aligned} P_b(e) &\leq \sum_{j+m=h_m}^{N/R_c^{i'}} e^{-\frac{(j+m)R_{SCCC}E_b}{N_0}} \\ &\cdot \sum_{w=w_m^{o'}}^{NR_c^{o'}} \sum_{l=d_f^{o'}}^N \sum_{j=d_f^{o''}}^{N/R_c^{o''}} \sum_{n^{o''}=1}^{n_M^{o''}} \sum_{n^{i'}=1}^{n_M^{i'}} N^{n^{o''}+n^{i'}-l-1} \frac{l!}{p^{n^{o''}+n^{i'}} n^{o''}! n^{i'}!} \frac{w}{R_c^{o'}} A_{w,l,j,n^{o''}}^{o''} A_{l,m,n^{i'}}^{i'} \end{aligned} \quad (8)$$

Equivalently, the upper bound for the frame error probability is given by

$$P_f(e) \leq \sum_{j+m=h_m}^{N/R_c^{i'}} e^{-\frac{(j+m)R_{\text{SCCC}}E_b}{N_0}} \cdot \sum_{w=w_m^o}^{NR_c^o} \sum_{l=d_f^o}^N \sum_{j=d_f^{o''}}^{N/R_c^{o''}} \sum_{n^{o''}=1}^{n_M^{o''}} \sum_{n^{i'}=1}^{n_M^{i'}} N^{n^{o''}+n^{i'}-l} \frac{l!l!}{p^{n^{o''}+n^{i'}} n^{o''}! n^{i'}!} A_{w,l,j,n^{o''}}^{o''} A_{l,m,n^{i'}}^{i'} \quad (9)$$

For large N and for a given $h = j + m$, the dominant coefficient of the exponentials in (8) and (9) is the one for which the exponent of N is maximum [8]. This maximum exponent is defined as

$$\alpha(h = j + m) \triangleq \max_{w,l} \{n^{o''} + n^{i'} - l - 1\} \quad (10)$$

For large E_b/N_0 , the dominating term is $\alpha(h_m)$, corresponding to the minimum value $h = h_m$,

$$\alpha(h_m) \leq 1 - d_f^{o'} \quad (11)$$

and the asymptotic bit error rate performance is given by

$$\lim_{E_b/N_0 \rightarrow \infty} P_b(e) \leq BN^{1-d_f^{o'}} \text{erfc} \left(\sqrt{\frac{h_m R_{\text{SCCC}} E_b}{N_0}} \right) \quad (12)$$

where B is a constant that depends on the weight properties of the encoders, and N is the interleaver length.

On the other hand, the dominant contribution to the bit and frame error probability for $N \rightarrow \infty$ is the largest exponent of N , defined as

$$\alpha_M \triangleq \max_h \alpha(h = j + m) = \max_{w,l,h} \{n^{o''} + n^{i'} - l - 1\} \quad (13)$$

We consider only the case of recursive convolutional inner encoders. In this case, α_M is given by

$$\alpha_M = - \left\lfloor \frac{d_f^{o'} + 1}{2} \right\rfloor \quad (14)$$

and

$$\lim_{N \rightarrow \infty} P_b(e) \leq KN^{\alpha_M} \text{erfc} \left(\sqrt{\frac{h(\alpha_M) R_{\text{SCCC}} E_b}{N_0}} \right) \quad (15)$$

where again K is a constant that depends on the weight properties of the encoders and $h(\alpha_M)$ is the weight associated to the highest exponent of N .

Now, denoting by $d_{f,\text{eff}}^{i'}$ the minimum weight of inner code C_i' sequences generated by input sequences of weight 2, we obtain the following results for the weight $h(\alpha_M)$ associated to the highest exponent of N :

$$\begin{aligned} h(\alpha_M) &= \frac{d_f^{o'} d_{f,\text{eff}}^{i'}}{2} + d^{o''}(d_f^{o'}) && \text{if } d_f^{o'} \text{ even} \\ h(\alpha_M) &= \frac{(d_f^{o'} - 3)d_{f,\text{eff}}^{i'}}{2} + h_m^{(3)} + d^{o''}(d_f^{o'}) && \text{if } d_f^{o'} \text{ odd} \end{aligned} \quad (16)$$

where $d^{o''}(d_f^{o'})$ is the minimum weight of C_o'' code sequences corresponding to a C_o' code sequence of weight $d_f^{o'}$ and $h_m^{(3)}$ is the minimum weight of sequences of the inner code C_i' generated by a weight-3 input sequence.

Finally, since $d^{o''}(d_f^{o'}) \geq d_f^{o''}$, we can also write

$$\begin{aligned} h(\alpha_M) &\geq \frac{d_f^{o'} d_{f,\text{eff}}^{i'}}{2} + d_f^{o''} && \text{if } d_f^{o'} \text{ even} \\ h(\alpha_M) &\geq \frac{(d_f^{o'} - 3)d_{f,\text{eff}}^{i'}}{2} + h_m^{(3)} + d_f^{o''} && \text{if } d_f^{o'} \text{ odd} \end{aligned} \quad (17)$$

From (15) and (16) we obtain the following result for the (asymptotic with respect N) bit error probability:

$$P_b(e) \leq C_{\text{even}} N^{-d_f^{o'}/2} \text{erfc} \left(\sqrt{\left(\frac{d_f^{o'} d_{f,\text{eff}}^{i'}}{2} + d^{o''}(d_f^{o'}) \right) \frac{R_{\text{SCCC}} E_b}{N_0}} \right) \quad (18)$$

if $d_f^{o'}$ is even, and

$$P_b(e) \leq C_{\text{odd}} N^{-\frac{d_f^{o'}+1}{2}} \text{erfc} \left(\sqrt{\left(\frac{(d_f^{o'} - 3)d_{f,\text{eff}}^{i'}}{2} + h_m^{(3)} + d^{o''}(d_f^{o'}) \right) \frac{R_{\text{SCCC}} E_b}{N_0}} \right) \quad (19)$$

if $d_f^{o'}$ is odd. Constants C_{even} and C_{odd} can be derived as in [8] for SCCC.

We observe that the coefficient $h(\alpha_M)$ increases with $d_{f,\text{eff}}^{i'}$, $d^{o''}(d_f^{o'})$ and also with $h_m^{(3)}$ in the case of odd $d_f^{o'}$. This suggests that, to improve the performance, one should choose a suitable combination of C_o'' and C_i' such that $h(\alpha_M)$ is maximized, and the puncturing patterns P_o , P' and P_i^p (and subsequently permeabilities ρ_s and ρ_p) should be selected accordingly. Moreover, such a combination depends on the value of $d_f^{o'}$. For instance, if $d_f^{o'} = 4$ the term $d_{f,\text{eff}}^{i'}$ appears to be dominant with respect to $d^{o''}(d_f^{o'})$, since it is multiplied by a factor two ($d_f^{o'}/2$), whereas for $d_f^{o'} = 2$ both contributions are equally weighted.

Notice also that the contribution of the code C_o'' to $h(\alpha_M)$, given by $d^{o''}(d_f^{o'})$, corresponds to the contribution of the inner code systematic part in Fig. 1. Therefore, since $d^{o''}(d_f^{o'})$ depends on

the outer code, to optimize the puncturing pattern P_i^s ($P_i^s = \Pi[P']$) of the inner code systematic bits, one must take into account this dependence.

We can draw from (18) and (19) some important design considerations:

- As for traditional SCCC, P_o should be chosen to optimize the outer code distance spectrum.
- The coefficient that multiplies the signal to noise ratio E_b/N_0 increases with $d_{f,\text{eff}}^{\prime}$ and $d^{\prime\prime}(d_f^{\prime})$. Thus, we deduce that P' and P_i^p should be chosen so that $h(\alpha_M)$ is maximized. This implies to select a suitable combination of permeabilities ρ_s and ρ_p . For a fixed pair ρ_s and ρ_p , P_i^p must be optimized to yield the best encoder \mathcal{C}'_i IOWEF. Furthermore, P' (i.e. P_i^s) must be selected to optimize $d^{\prime\prime}(d_f^{\prime})$. If we consider (16) instead of (17), the criterion is equivalent to optimize the distance spectrum of \mathcal{C}''_o . Notice that this is equivalent to optimize the outer code \mathcal{C}_o punctured through P_o and P' with permeability ρ_s . Then, P_i^s must be set to the interleaved version of P' , i.e., $P_i^s = \Pi[P']$. Therefore, P_i^s turns out to depend on the outer code, and thus, it is also interleaver dependent. We stress the need to optimize P_i^s according to this dependence.

A complementary analysis tool for the design of concatenated schemes would be to consider the EXIT charts or equivalent plots [15,16]. These analysis techniques explain very well the behavior of iterative decoding schemes in the low SNR region (convergence region) and often lead to design rules that are in contrast with those outlined in this section, which are more suited for the analysis in the error floor region. Unfortunately, EXIT chart analysis is mainly based on Monte Carlo simulations and does not allow to extract useful code design parameters. For this reason we have not included this technique in the paper. The reader however should be warned that for the careful design of concatenated schemes both aspects must be considered and this implies that comparison of the designed schemes through simulation cannot be avoided. This fact also allows to justify some differences in the simulation results which are not evident from the uniform interleaver analysis. A convergence analysis of this class of SCCC will be discussed in a forthcoming paper.

IV. RATE-COMPATIBLE SERIAL CONCATENATED CONVOLUTIONAL CODES

Rate-compatible serial concatenated convolutional codes are obtained by puncturing inner code bits with the constraint that all the code bits of a high rate code must be kept in all lower rate codes. Depending on the puncturing pattern, the resulting code may be systematic (none

of the systematic bits are punctured), partially systematic (a fraction of the systematic bits are punctured) or non-systematic (all systematic bits are punctured). In [9] it was argued that a systematic inner code performs better than a partially systematic code. This result was assumed in [4] and [10] to build rate-compatible SCCCs limiting puncturing to inner parity bits. This assumption, however, is not valid for all SNRs. Indeed, keeping some systematic bits may be beneficial for speed up iterative decoding convergence. Since puncturing is limited to inner parity bits, the rate of the SCCC satisfies the constraint $R_{\text{SCCC}} \leq R_c'$. As already stated, in contrast to [4] and [10] we do not restrict puncturing to parity bits, but extend it also to systematic bits, thus allowing R_{SCCC} beyond the outer code rate R_c' , which provides a higher flexibility.

Assuming an outer encoder puncturing pattern fixed (P_o in Fig. 1), the design of well-performing rate-compatible SCCCs in the form of Fig. 1 limits to optimize the inner code puncturing patterns for systematic and parity bits according to the design criteria outlined in the previous section, with the constraint of rate-compatibility. Applying these design rules, optimal SCCC families can be found considering inner systematic and inner parity bits separately:

- To find the optimum puncturing pattern for inner code parity bits, start puncturing the inner mother code parity bits one bit at a time, fulfilling the rate-compatibility restriction. Define as d_w the minimum weight of inner codewords generated by input words with weight w , and by N_w the number of nearest neighbors (multiplicities) with weight d_w . Select at each step the candidate puncturing pattern P_i^p for the inner code parity bits as the one optimizing its IOWEF, i.e., yielding the optimum values for (d_w, N_w) for $w = 2, \dots, w_{max}$ (first d_w is maximized and then N_w is minimized).
- Select the candidate puncturing pattern P' as the one yielding the best outer code (punctured through P_o and P') output weight enumerating function (OWEF). Namely, to find the optimum puncturing pattern for inner code systematic bits, start puncturing the outer mother code output bits one bit at a time, fulfilling the rate-compatibility restriction.

Define as A_d the number of nearest neighbors (multiplicities) with output distance d of the outer code. Select at each step the candidate puncturing pattern P' as the one yielding the optimum values for A_d , i.e., the one which sequentially optimize the values A_d for

$d = d_{\text{free}}, \dots, d_{\text{max}}$. Since also outer code information bits are punctured, the invertibility³ of the outer code at each step must be guaranteed. At the end, since the systematic bits at the input of the inner encoder are an interleaved version of the outer encoder output bits, take the best puncturing pattern P' and apply its interleaved version $P_i^s = \Pi[P']$ to inner code systematic bits (see Figs. 1 and 2).

V. SIMULATION RESULTS AND COMPARISON WITH ANALYTICAL BOUNDS

The performance of rate-compatible SCCCs mainly depend on its overall rate R_{SCCC} and on the selected combination of ρ_s and ρ_p . In this Section, based on the considerations drawn in Section III and IV, we discuss how to properly select ρ_s and ρ_p . We compare through simulation several rate-compatible puncturing schemes, with different interleaver lengths, and compare the performance of the proposed codes with the upper bounds to the error probability.

We consider the serial concatenation of two rate-1/2, 4-states, systematic recursive encoders, with generator polynomials (1, 5/7) in octal form. The outer encoder is punctured to rate 2/3 by applying a fixed puncturing pattern. In particular, two puncturing patterns P_o have been taken into account, namely $P_{o,1} = \begin{bmatrix} 1 & 1 \\ 1 & 0 \end{bmatrix}$ and $P_{o,2} = \begin{bmatrix} 1 & 1 & 1 & 1 \\ 1 & 1 & 0 & 0 \end{bmatrix}$. The overall code rate is, thus, $R_{\text{SCCC}} = 1/3$. Higher rates are then obtained by puncturing the inner encoder through puncturing patterns P_i^s and P_i^p for systematic and parity bits, respectively, as previously discussed. The free distance of the outer encoder, $d_f^{o'}$, when puncturing pattern $P_{o,1}$ is applied, is odd and equal to 3, whereas for $P_{o,2}$, $d_f^{o'}$ is even and equal to 4. Some considerations must be done at this point:

- 1) If $d_f^{o'} = 3$, $\alpha_M = -\left\lfloor \frac{d_f^{o'} + 1}{2} \right\rfloor = -2$. In this case, the minimum weight of inner code input sequences that yields $\alpha_M = -2$ (since $n^{o''} = n^{i'} = 1$) is $l_{\text{min}} = 3$, and $h(\alpha_M) = h_m^{(3)} + d^{o''}(d_f^{o'})$. However, this value of α_M is achieved also by the inner input weights $l = 4$ and $l = 6$, leading to a slight modification of (16). In fact, $l = 4$ yields $\alpha_M = -2$ (since $n^{o''} = 1$ and $n^{i'} = 2$), and $h(\alpha_M) = 2d_{f,\text{eff}}^i + d^{o''}(d_f^{o'} + 1)$. Also $l = 6$ yields $\alpha_M = -2$ (since $n^{o''} = 2$ and $n^{i'} = 3$), and $h(\alpha_M) = 3d_{f,\text{eff}}^i + 2d^{o''}(d_f^{o'})$. Notice that even when $l > l_{\text{min}}$ yields the maximum value of $\alpha_M = -2$, the design rules stated in Section IV are still valid, leading in every case to the maximization of $h(\alpha_M)$.

³A code is said to be invertible if, knowing only the parity-check symbols of a code vector, the corresponding information symbols can be uniquely determined [11].

- 2) If $d_f^{o'} = 4$, $\alpha_M = -\left\lfloor \frac{d_f^{o'}+1}{2} \right\rfloor = -2$. In this case, only the minimum weight of the inner code input sequences $l_{\min} = 4$ yields $\alpha_M = -2$ (since $n^{o''} = 1$ and $n^{i'} = 2$), and $h(\alpha_M) = 2d_{f,\text{eff}}^{i'} + d_f^{o''}$.

The algorithm to find the optimal (where optimal is intended to be according to the criterion addressed in Section IV) puncturing patterns P_i^p and $P_i^s = \Pi[P']$ for inner code parity and systematic bits, respectively, works sequentially, by puncturing one bit at a time in the optimal position, subject to the constraint of rate compatibility. This sequential puncturing is performed starting from the lowest rate code (i.e., the baseline rate-1/3 code), and ending up at the highest possible rate. In Table I the puncturing pattern P_i^p for inner code parity bits is shown. To find this pattern, a frame length $K = 200$ and an interleaver length $N = K/R_c^{o'} = 300$ have been assumed. The puncturing pattern has been found by optimizing the inner code IOWEF, as explained in the previous section. This puncturing pattern yields the optimum values of (d_w, N_w) for $w = 2, \dots, w_{\max}$ and for each puncturing position. The puncturing positions of P_i^p go from 1 to the interleaver length N . The evolution of the values (d_w, N_w) with the number of punctured inner parity bits for $w = 2$ are reported in Fig. 3. Notice that $d_w, \forall w$ (not only for $w = 2$), is a non-increasing function of the number of punctured bits, and there are some $d_w = 0$ with a corresponding $N_w \neq 0$, which means that the corresponding code C_i' is not invertible. Notice also that N_2 , given a value of d_2 , is an increasing function of the number of punctured bits.

In Table II the puncturing pattern P' , the interleaved version of which, $\Pi[P']$, is meant for inner code systematic bits, is shown, having applied the fixed puncturing pattern $P_{o,1}$ to the outer code. This puncturing pattern yields the best outer code (punctured through $P_{o,1}$ and P') output weight enumerating function (OWEF) for each puncturing position. The puncturing positions go from 1 to $2K$, being K the frame length. The number of punctured bits go from 0 to $K/2$, i.e., the rate of the outer code punctured through $P_{o,1}$ and P' is assumed to go from $2/3$ (no puncturing is applied to the systematic bits) to 1. The reason to limit the rate of C_o'' up to 1 is that further puncturing results in a significant performance degradation. The puncturing pattern P' for inner code systematic bits having applied $P_{o,2}$ is shown in Table III.

We have also performed an optimization of the inner code systematic bits puncturing pattern $P_i^s = \Pi[P']$ restricting the puncturing to outer code parity bits only, thus yielding to an overall systematic SCCC. The puncturing pattern P' , having applied the fixed puncturing pattern $P_{o,1}$ to

systematic bits, is reported in Table IV. It is worth to point out that the performances obtained by restricting the puncturing to outer code systematic bits are very similar to those obtained without this restriction.

In Table V are listed the parameters $h_m^{(3)}$, $d^{o''}(d_f^{o'})$, $h(\alpha_M)$, h_m and the multiplicity N_{h_m} of the codewords at distance h_m , for different values of the parity permeability ρ_p for an SCCC of overall code rate $R_{\text{SCCC}} = 2/3$, being the outer encoder punctured through $P_{o,1}$, and the inner encoder punctured through P_i^p , reported in Table I, and $P_i^s = \Pi[P']$, where P' is reported in Table II. Notice that being $R_c^{o'} = 2/3$ in (2), to obtain a rate $R_{\text{SCCC}} = 2/3$ code ρ_s and ρ_p must be related by

$$\rho_s = 1 - \rho_p \quad (20)$$

For instance, the code with $\rho_p = 20/300$ has been obtained by applying the puncturing pattern of Table I to inner code parity bits, selecting the first $280 = N(1 - \rho_p)$ puncturing positions in Table I, and applying the interleaved version of the puncturing pattern of Table II to inner code systematic bits, selecting the first $20 = N(1 - \rho_s)$ puncturing positions in Table II, so that $\rho_s + \rho_p = 1$ (see (20)).

The frame length selected for this example is $K = 200$. The corresponding interleaver length N is given by $K/R_c^{o'} = 300$. The different values of ρ_p are listed as rational numbers with denominator N (since the maximum number of inner parity bits which are not punctured is N). For all permeabilities $h_m^{(3)} = 0$, thus $h(\alpha_M)$ is completely dominated by $d^{o''}(d_f^{o'})$.

The union bound (9) on the residual Frame Error Rate (FER) of the codes listed in Table V is plotted in Fig. 4. The markers used in Fig. 4 correspond to those listed in Table V. It is shown that the error floor is lowered by increasing ρ_p , i.e., the proportion of surviving inner code parity bits. The higher error floor is obtained for $\rho_p = 20/300$, whereas increasing ρ_p leads to better performance in the error floor region. Nevertheless, it should be stressed that a sufficient number of systematic bits should be preserved in order to ensure a good behavior for high E_b/N_0 values. This can be observed for the curve $\rho_p = 100/300$, which shows a worse slope. Indeed, for asymptotic values of E_b/N_0 , the performance is dominated by h_m , the minimum weight of code sequences. Therefore, the best performance for very high signal-to-noise ratios E_b/N_0 is obtained for $\rho_p = 20/300$ (curve with '□' in Fig. 4), since the corresponding code has $h_m = 3$, whereas the worst performance is obtained for $\rho_p = 100/300$ (curve with 'o' in Fig. 4), since

the corresponding code has $h_m = 1$.

In Fig. 5 we compare simulation results of the rate-2/3 SCCC of Table V with the analytical upper bounds for several values of ρ_p . The curves are obtained with a *log-map* SISO algorithm and 10 decoding iterations. These results are obtained considering a random interleaver of length $N = 3000$ and applying the puncturing patterns of Tables I and II periodically. The simulation results show a very good agreement with the analytical bounds and confirm that lower error floors can be obtained by increasing ρ_p . For example, the code $\rho_p = 8/30$ shows a gain of 1.4 dB at FER= 10^{-5} w.r.t. the code $\rho_p = 2/30$. Howeverm this gain tends to vanish for very high E_b/N_0 , where the term h_m is predominant (note the of the two curves).

On the other hand, the performance in the waterfall region can be explained in part looking at the cumulative function $\sum_1^d A_h^{C_s}$ of the output distance spectrum of the serial concatenated codes. The codes for which the cumulative function of the average distance spectrum is minimum perform better at low SNRs, since, in this region, the higher distance error events have a nontrivial contribution to error performance. The cumulative functions of the codes listed in Table V are traced in Fig. 6. The worst performance for low signal-to-noise ratios E_b/N_0 is obtained for $\rho_p = 20/300$ (curve with '□' in Fig. 4), since the corresponding code has the maximum cumulative function of the average distance spectrum, whereas the best performance is obtained for $\rho_p = 100/300$ (curve with 'o' in Fig. 4), since the corresponding code has the minimum cumulative function of the average distance spectrum. This is in agreement with the simulation results of Fig. 5.

For comparison purposes, we also report in Fig. 5 the performance of the rate-2/3 PCCC proposed in [12] and the rate-2/3 SCCC proposed in [4]. The PCCC code in [12] is a code of similar complexity of the SCCC codes proposed here obtained by optimally puncturing the mother code specified in the wideband code-division multiple-access (WCDMA) and CDMA2000 standards, consisting of the parallel concatenation of two rate-1/2, 8-states, convolutional encoders. The SCCC code in [4] is the same as our baseline code (two rate-1/2, 4-states, systematic recursive encoders), but puncturing is limited to inner code parity bits. As it can be observed in Fig. 5, the proposed SCCC code shows a significant gain in the error floor region w.r.t. the code in [12]. On the other hand, the code in [4] performs much worse than our code, since all inner code systematic bits are maintained after puncturing.

In Table VI are listed the parameters $d_{f,\text{eff}}^{i'}$, $d^{o''}(d_f^{o'})$, $h(\alpha_M)$, h_m and the multiplicity N_{h_m}

of the codewords at distance h_m , for different values of ρ_p , being the outer encoder punctured through P_i^p , reported in Table I, and $P_i^s = \Pi[P']$, where P' is reported in Table III. The frame length selected for this example is always $K = 200$ ($N = 300$).

Fig. 7 gives the union bound (9) on the residual Frame Error Rate of the codes listed in Table VI. The markers used in Fig. 7 are listed in Table VI. Similar performance to the codes of Fig. 4 (obtained applying $P_{o,1}$ and the puncturing patterns of Tables I and III) are observed. The bounds are congruent with the parameters reported in Table VI. All the codes with $\rho_p > 20/300$ have $h(\alpha_M) = h_m = 2$. Then, the performance are dominated by the multiplicity of N_{h_m} which diminishes as ρ_p increases, i.e., the number of inner code parity bits which are not punctured is increased. Therefore, to enhance performance in the error floor region one should put more puncturing on inner code systematic bits. In fact, the hierarchy of the curves in Fig. 7 corresponds to the hierarchy of N_{h_m} in Table VI. Finally, the curve corresponding to $\rho_p = 20/300$ shows the worst performance in the region of interest, where the multiplicity N_{h_m} is the dominant term. However, for very high E_b/N_0 , being the performance mainly dominated by h_m (equal to three), the curve corresponding to $\rho_p = 20/300$ shows the best performance.

Fig. 8 shows the simulated performance of the SCCCs with rate $R_{\text{SCCC}} = 9/10$ in terms of residual FER vs. $R_{\text{outer}} = K\rho_s$, for different values of E_b/N_0 . The curves show that the higher the SNR, and hence the lower the target FER, the heavier should be the puncturing on inner systematic bits, i.e., the lower should be ρ_s . On the contrary, for higher error probabilities it is advantageous to keep more systematic bits.

Finally, in Fig. 9 we compare the simulated performance of the SCCCs with rate $R_{\text{SCCC}} = 9/10$ with the analytical upper bounds for several values of ρ_p . The curves show that the higher the E_b/N_0 , the heavier should be the puncturing on inner systematic bits, i.e., the higher should be ρ_p . Nevertheless, it should be stressed that some of the inner systematic bits must be maintained in order to allow convergence of the decoding process. For comparison purposes, we also report in the same figure the performance of the rate-9/10 PCCC proposed in [12]. A gain of 2 dB at FER 10^{-5} is obtained for the code $\rho_p = 160/2220$ w.r.t. the code in [12].

From the analytical upper bounds and these examples we may conclude that performance strongly depend on the puncturing patterns, and also on the spreading of the puncturing over the inner code systematic bits and parity bits. To lower the error floor, it is advantageous to put more puncturing on inner code systematic bits, resulting in a lower error floor and, in general,

in a faster convergence (see the curves marked with filled circles in Fig. 5).

VI. CONCLUSIONS

In this paper we have proposed a method for the design of rate-compatible serial concatenated convolutional codes (SCCC).

To obtain rate-compatible SCCCs, the puncturing has not been limited to inner parity bits only, but has also been extended to inner systematic bits, puncturing the inner encoder beyond the unitary rate. A formal analysis has been provided for this new class of SCCC by deriving the analytical upper bounds to the error probability. Based on these bounds, we have derived suitable design guidelines for this particular code structure to optimize the inner code puncturing patterns. In particular, it has been shown that the puncturing of the inner code systematic bits depends on the outer code and, therefore, it is also interleaver dependent. Moreover, the performance of a SCCC for a given rate can be enhanced in the error-floor region by increasing the proportion of surviving inner code parity bits, as far as a sufficient number of systematic bits is preserved.

The code analyzed in this paper, due to its simplicity and versatility, has been chosen for the implementation of a very high speed (1Gbps) Adaptive Coded Modulation modem for satellite application. The interested reader can find implementation details in [17].

REFERENCES

- [1] J. Hagenauer, *Rate-compatible punctured convolutional codes (RCPC codes) and their applications*, IEEE Trans. Comm., vol. 36, pp. 389-400, April 1988.
- [2] C. Berrou and A. Glavieux, *Near Optimum Error Correcting Coding and Decoding: Turbo-codes*, IEEE Trans. Comm., vol. 44, n. 2, pp. 1261-1271, Oct. 1996,.
- [3] A. S. Barbulescu, and S. S. Pietrobon, *Rate Compatible Turbo Codes*, IEEE Electronic Letters, vol. 31, no. 7, pp. 535-536, Mar. 1995.
- [4] H. Kim, and G. L. Stüber, *Rate Compatible Punctured SCCC*, in Proc. IEEE 54th Vehic. Techn. Conf., VTC'01-Fall, pp. 2399-2403, Oct. 2001.
- [5] N. Chandran, and M.C. Valenti, *Bridging the Gap between Parallel and Serial Concatenated Codes*, in Proc. Virginia Tech. Symp. on Wir. Pers. Comm., pp. 145-154, June 2002.
- [6] F. Babich, G. Montorsi and F. Vatta, *Design of Rate-Compatible Punctured Serial Concatenated Convolutional Codes*, in Proc. IEEE Int. Conf. Comm., ICC 2004, pp. 552-556, June 2004.
- [7] S. Benedetto, and G. Montorsi, *Unveiling Turbo Codes: Some Results on Parallel Concatenated Coding Schemes*, IEEE Trans. Inf. Theory, vol. 42, pp. 409-429, Mar. 1996.
- [8] S. Benedetto, D. Divsalar, G. Montorsi, and F. Pollara, *Serial Concatenation of Interleaved Codes: Performance Analysis, Design, and Iterative Decoding*, IEEE Transactions on Information Theory, vol. 44, no. 3, pp. 909-926, May 1998.

- [9] O. F. Açikel, and W. E. Ryan, *Punctured High Rate SCCCs for BPS/QPSK Channels*, in Proc. IEEE Int. Conf. Comm., GLOBECOM'00, vol. 1, pp. 434-439, Mar. 2000.
- [10] N. Chandran, and M. C. Valenti, *Hybrid ARQ using serial concatenated convolutional codes over fading channels*, in Proc. IEEE 53rd Vehic. Tech. Conf., VTC'01-Spring, vol. 2, pp. 1410-1414, May 2001.
- [11] S. Lin and D. J. Costello, Jr., "Error control coding, fundamentals and applications", *Prentice-Hall, Inc.*, New Jersey, 1983.
- [12] F. Babich, G. Montorsi and F. Vatta, "Some Notes on Rate-compatible Punctured Turbo Codes (RCPTC) Design", *IEEE Trans. on Comm.*, vol. 52, no. 5, pp. 681-684, May 2004.
- [13] S. Benedetto and G. Montorsi, *Design of Parallel Concatenated Convolutional Codes*, IEEE Transactions on Communications, vol. 44, No. 5, pp. 591-600, May 1996.
- [14] D. N. Rowitch and L. B. Milstein, "On the performance of hybrid FEC/ARQ systems using rate compatible punctured turbo (RCPT) codes", *IEEE Transactions on Communications*, Vol. 48, No. 6, June 2000, pp. 948-959.
- [15] S. ten Brink, "Design of Concatenated Coding Schemes Based on Iterative Decoding Convergence", *Ph.D Dissertation, Institute of Telecommunications, University of Stuttgart. April 2001*
- [16] D. Divsalar, S. Dolinar, and F. Pollara "Iterative Turbo Decoder Analysis Based on Density Evolution", *IEEE Jour. Sel. Areas in Comm.*, vol. 19, no. 5, May 2001.
- [17] S. Benedetto, R. Garello, G. Montorsi, C. Berrou, C. Douillard, D. Giancristofaro, A. Ginesi, L. Giugno, M. Luise, *Modulation, coding and signal processing for wireless communications - MHOMS: high-speed ACM modem for satellite applications*, IEEE Wireless Communications, vol. volume 12, no. 2, pp. 66 - 77, April 2005.

LIST OF FIGURES

1	Block diagram of the Serial concatenated code scheme.	20
2	Modified block diagram of the serial concatenated scheme.	21
3	Inner code effective free distance d_2 (thick line) and its multiplicity N_2 (thin line) as a function of the	
4	Union bound performance of the rate $2/3 R_{SCCC}$ in terms of residual FER versus E_b/N_0 with $N = 3000$	
5	Simulation results and performance bounds of the rate $2/3 R_{SCCC}$ with $N = 3000$. The performances of	
6	The cumulative function $\sum_1^d A_h^{C_s}$ of the distance spectra of the rate $2/3 R_{SCCC}$ codes obtained applying	
7	Union bound performance of the rate $2/3 R_{SCCC}$ in terms of residual FER versus E_b/N_0 with $N = 3000$	
8	FER performance versus $R_{outer} = K\rho_s$ for several E_b/N_0 . Rate-9/10 SCCC. N=3000. 27	
9	Simulation results and performance bounds of the rate 9/10 R_{SCCC} with $N = 3000$. The performances	

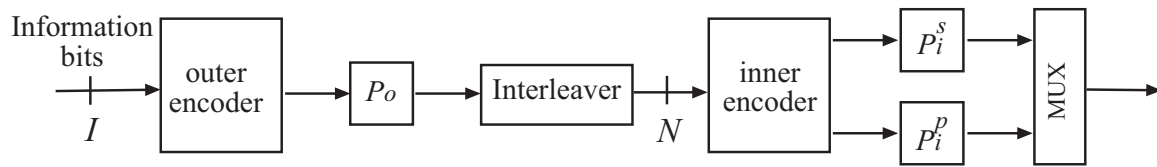


Fig. 1. Block diagram of the Serial concatenated code scheme.

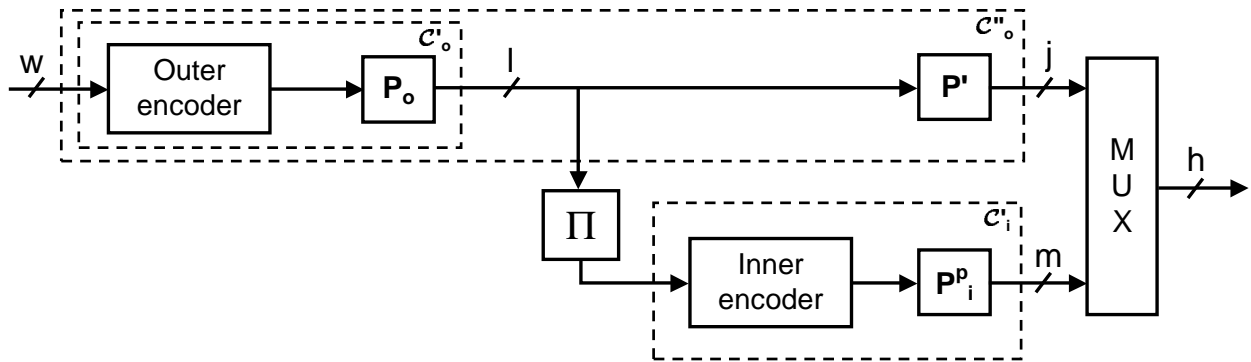


Fig. 2. Modified block diagram of the serial concatenated scheme.

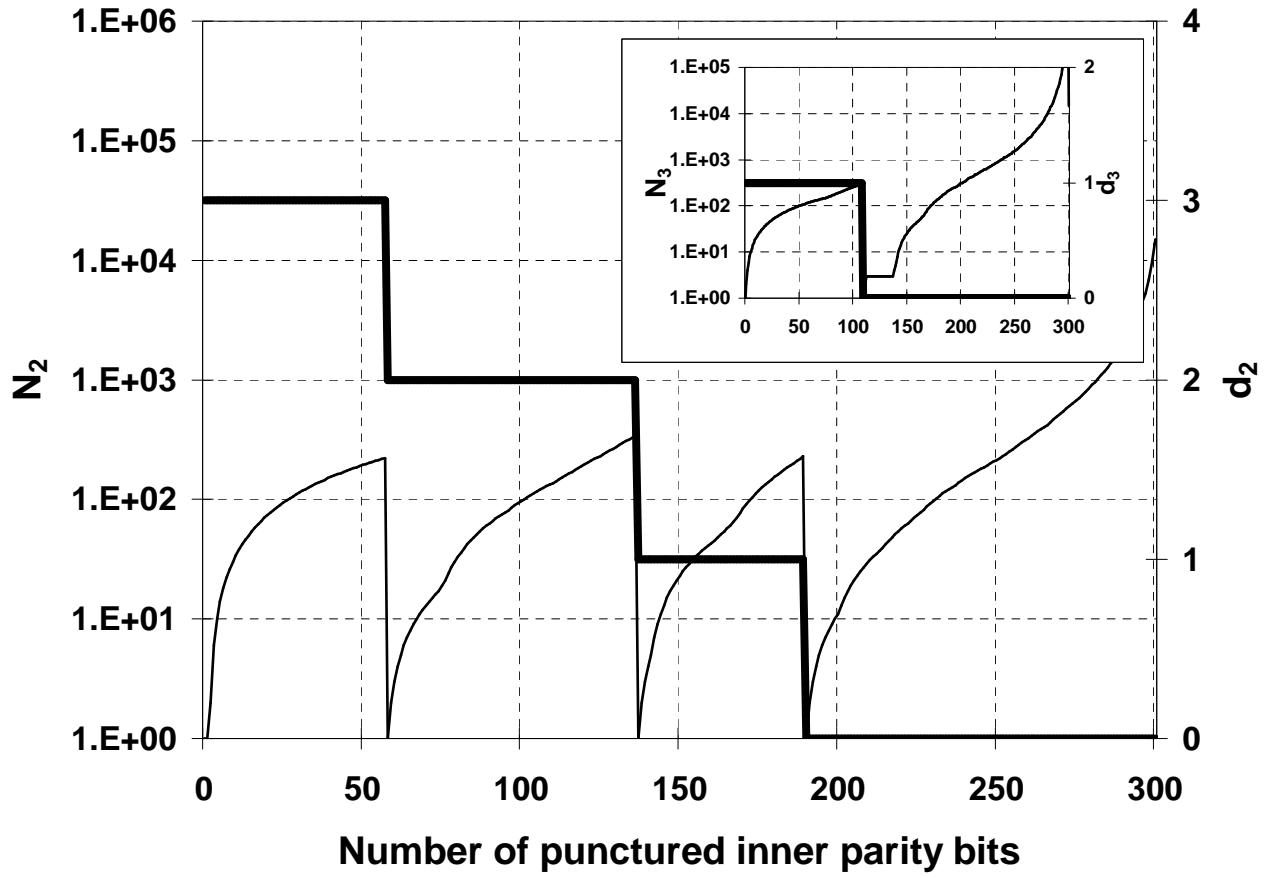


Fig. 3. Inner code effective free distance d_2 (thick line) and its multiplicity N_2 (thin line) as a function of the number of punctured inner parity bits.

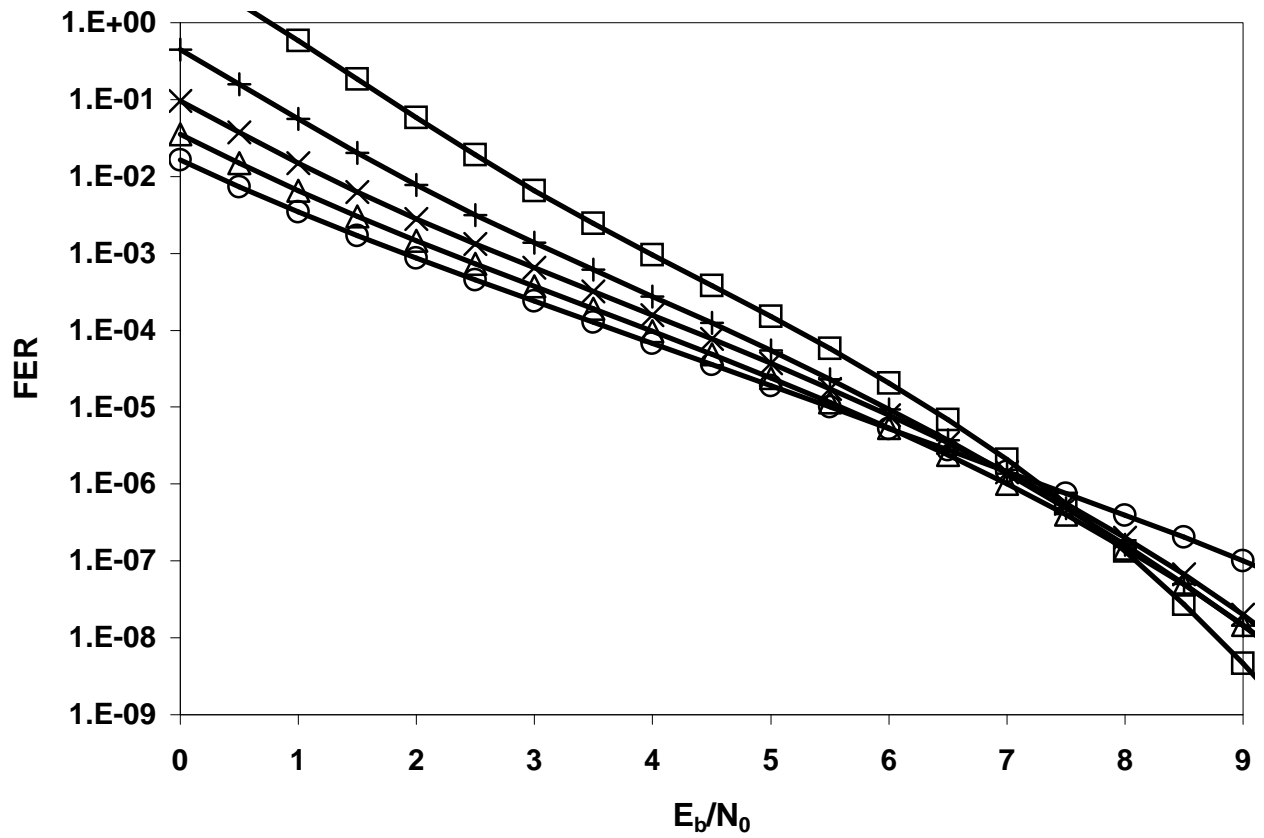


Fig. 4. Union bound performance of the rate $2/3 R_{\text{SCCC}}$ in terms of residual FER versus E_b/N_0 with $N = 300$. The performances obtained applying the different ρ_p values listed in Table V are shown. The corresponding markers are also listed in Table V.

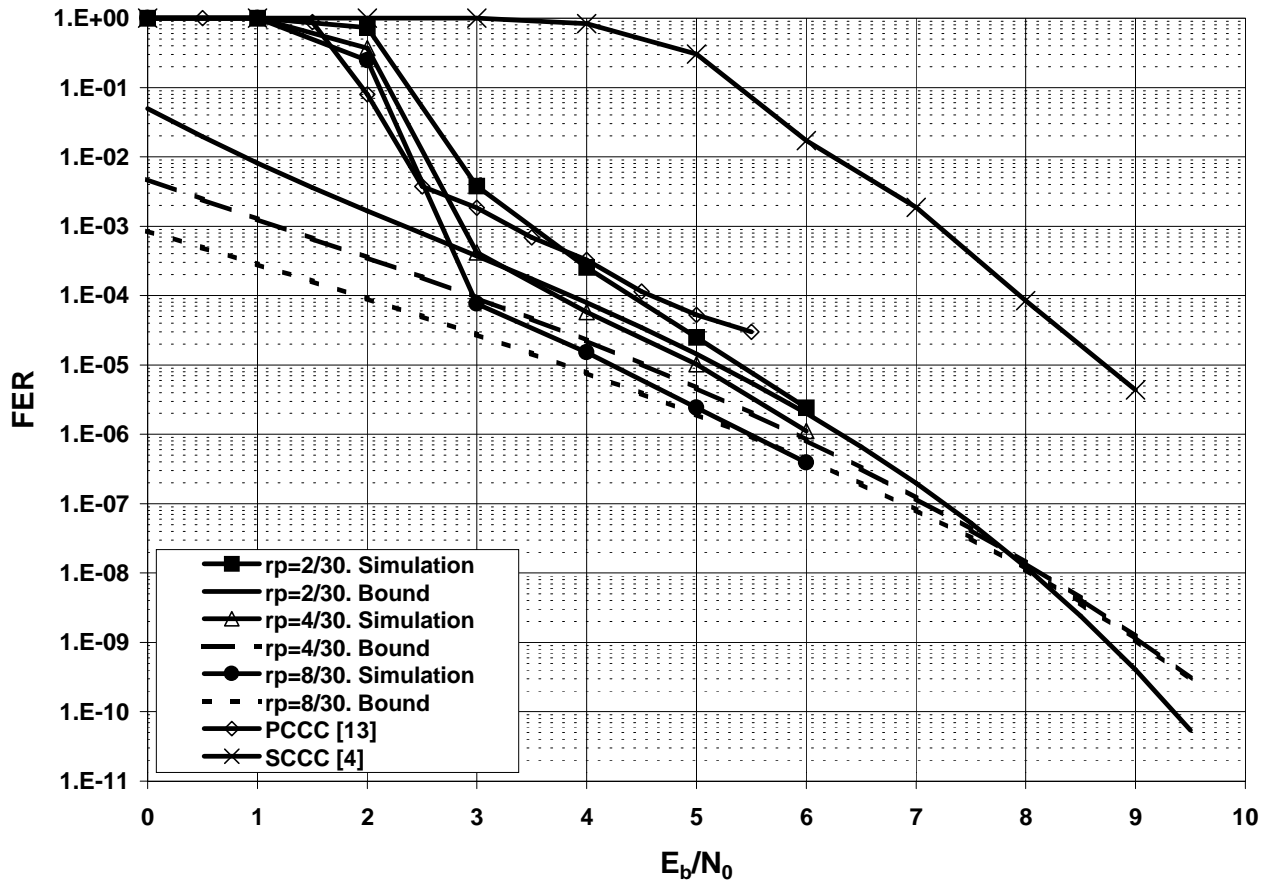


Fig. 5. Simulation results and performance bounds of the rate $2/3 R_{SCCC}$ with $N = 3000$. The performances obtained applying the different ρ_p values listed in Table V are shown.

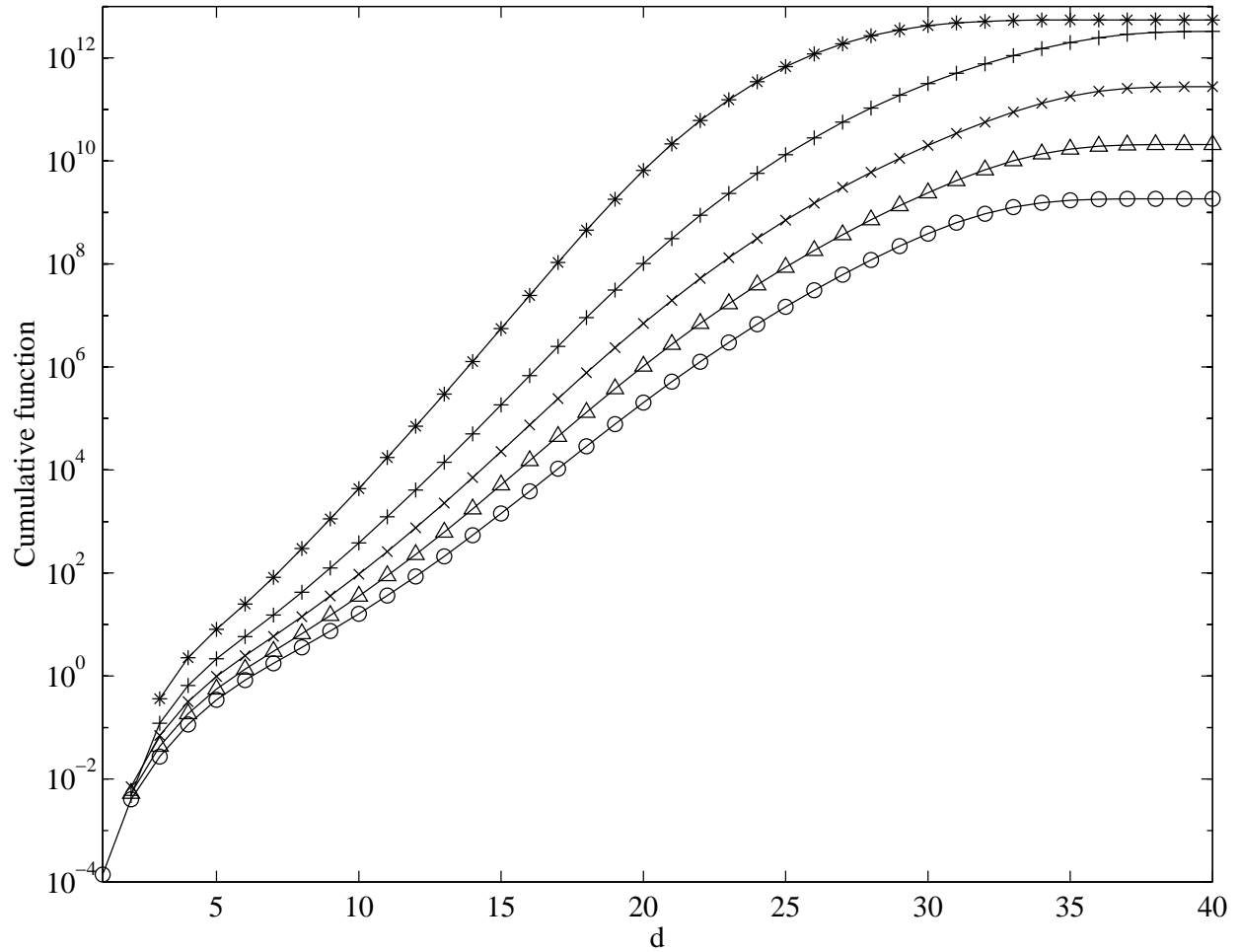


Fig. 6. The cumulative function $\sum_1^d A_h^{C_s}$ of the distance spectra of the rate $2/3$ R_{SCCC} codes obtained applying the different ρ_p values listed in Table V. The corresponding markers are also listed in Table V.

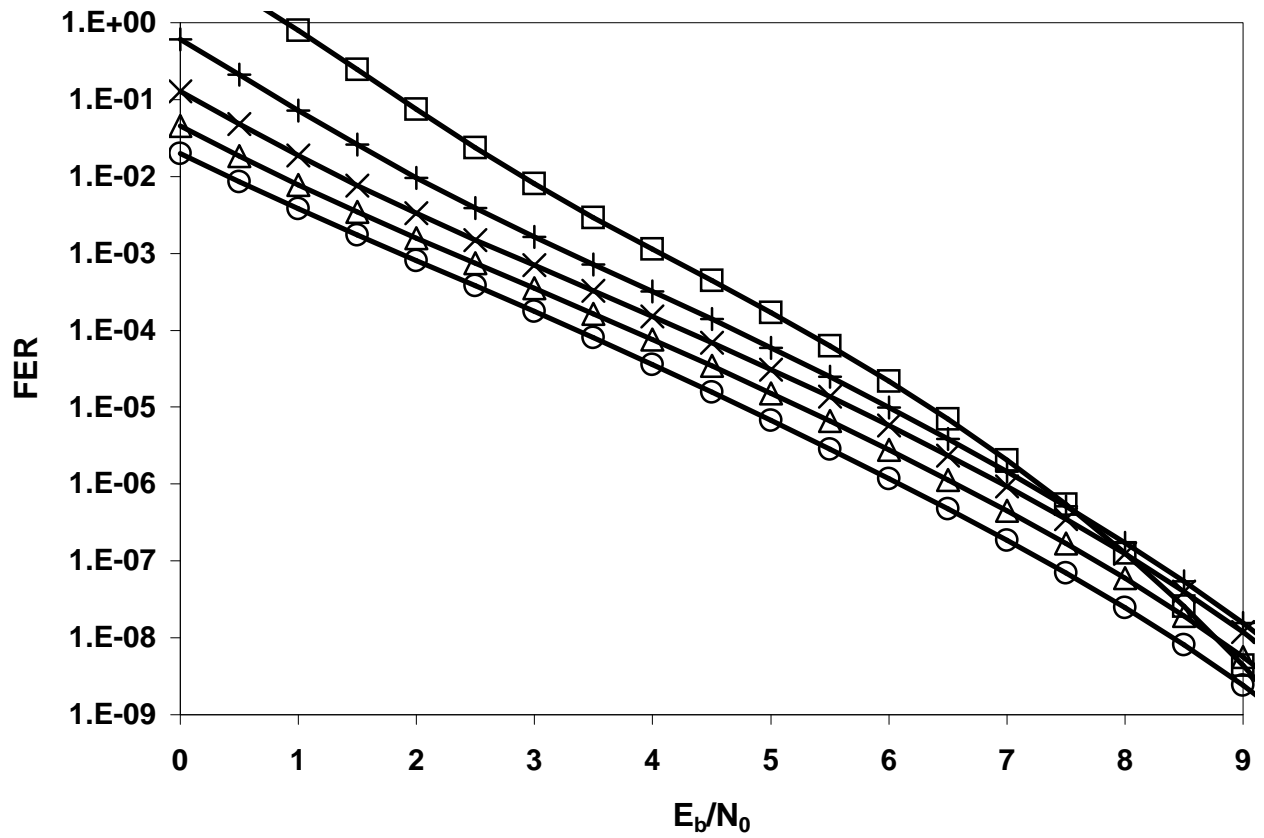


Fig. 7. Union bound performance of the rate $2/3 R_{\text{SCCC}}$ in terms of residual FER versus E_b/N_0 with $N = 300$. The performances obtained applying the different ρ_p values listed in Table VI are shown. The corresponding markers are also listed in Table VI.

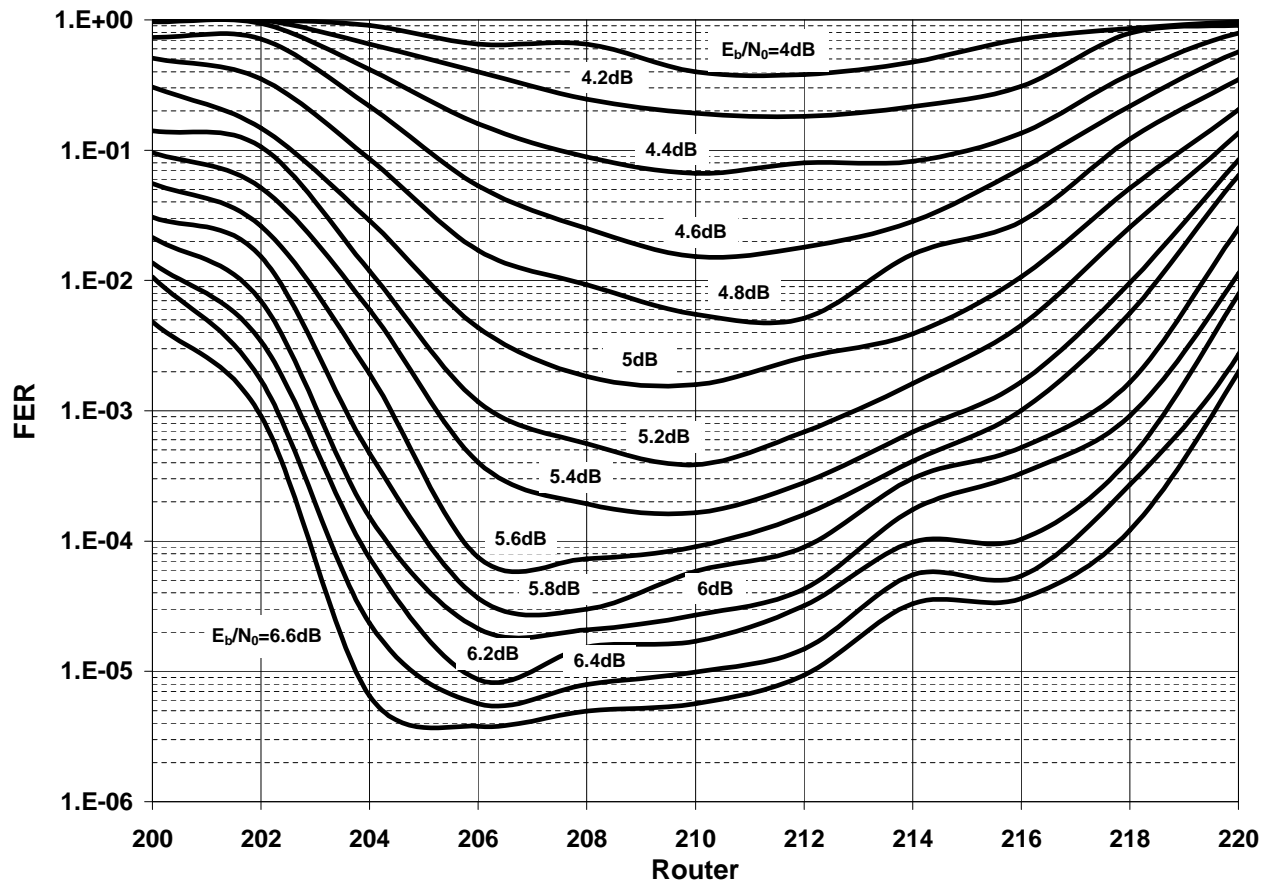


Fig. 8. FER performance versus $R_{outer} = K\rho_s$ for several E_b/N_0 . Rate-9/10 SCCC. N=3000.

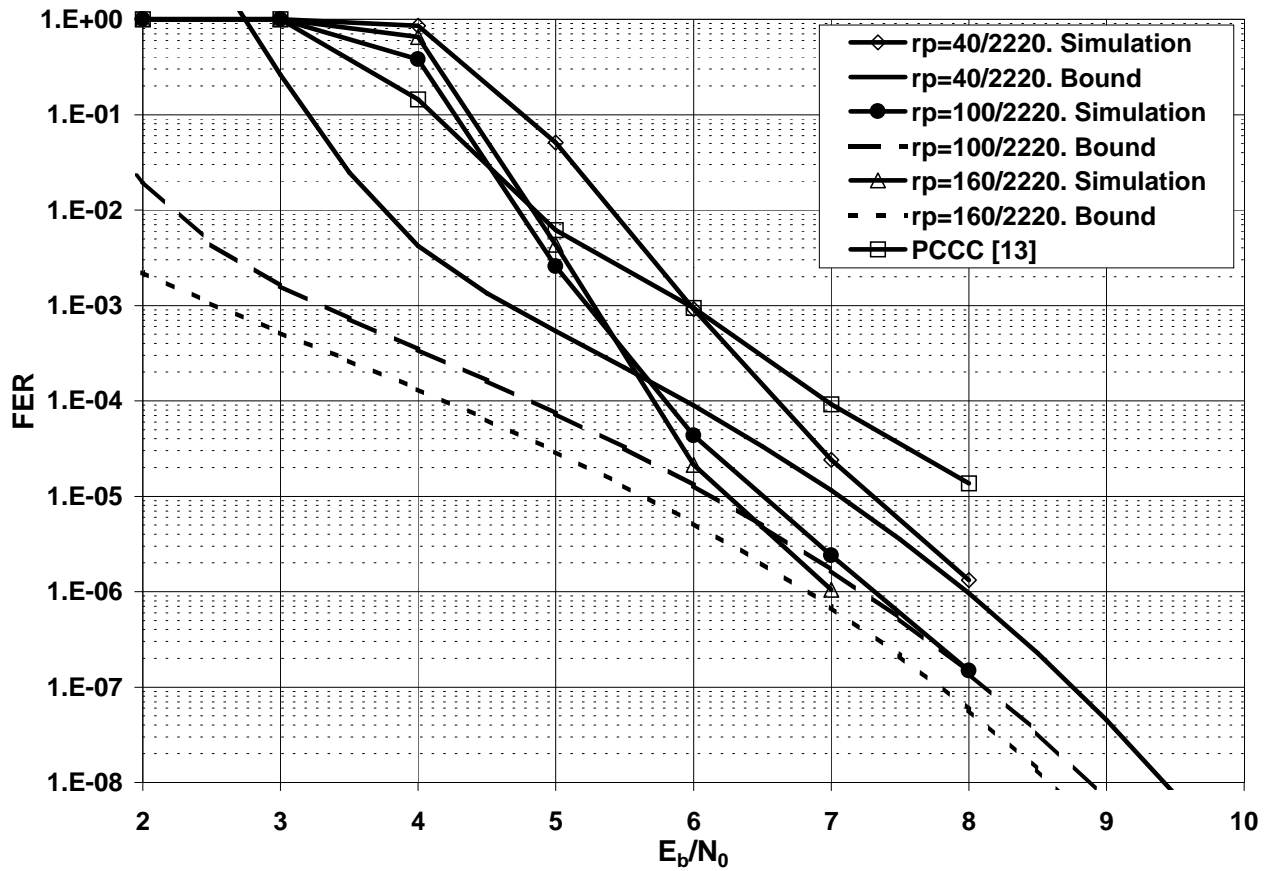


Fig. 9. Simulation results and performance bounds of the rate $9/10 R_{\text{SCCC}}$ with $N = 3000$. The performances obtained applying the different ρ_p values listed in Table V are shown.

LIST OF TABLES

I Puncturing positions for inner code parity bits. 30

II Puncturing positions for inner code systematic bits and fix puncturing pattern $P_{o,1}$. 31

III Puncturing positions for inner code systematic bits and fix puncturing pattern $P_{o,2}$. 32

IV Puncturing positions for inner code systematic bits corresponding to outer code parity bits and fix puncturing pattern $P_{o,1}$. 33

V Parameters of the rate $R_{SCCC} = 2/3$ code with interleaver length N and the first fix puncturing pattern $P_{o,1}$. 34

VI Parameters of the rate $R_{SCCC} = 2/3$ code with interleaver length N and the second fix puncturing pattern $P_{o,2}$. 35

TABLE I
PUNCTURING POSITIONS FOR INNER CODE PARITY BITS.

Index	Puncturing position									
1 - 10	299	0	5	294	276	77	96	257	139	24
11 - 20	47	224	264	126	54	151	17	174	192	106
21 - 30	161	241	212	89	250	36	283	113	236	63
31 - 40	205	82	269	68	217	31	229	179	144	12
41 - 50	156	101	131	187	169	118	200	289	42	245
51 - 60	73	58	165	135	122	196	183	279	260	21
61 - 70	51	298	92	1	220	253	233	148	28	209
71 - 80	110	272	85	9	286	39	64	157	102	173
81 - 90	140	127	191	240	72	117	201	46	265	225
91 - 100	16	249	81	213	32	290	180	57	95	166
101 - 110	147	232	109	8	275	25	256	88	282	133
111 - 120	206	186	153	295	221	43	268	35	123	69
121 - 130	244	195	78	162	50	4	143	20	105	170
131 - 140	114	216	237	261	13	228	130	136	60	177
141 - 150	98	203	287	184	252	91	159	66	273	120
151 - 160	75	55	29	40	210	198	84	280	189	247
161 - 170	292	150	99	176	61	154	3	297	230	18
171 - 180	263	111	219	141	167	48	239	125	11	193
181 - 190	70	34	271	254	208	79	103	285	182	138
191 - 200	227	164	22	45	242	128	115	94	52	145
201 - 210	6	267	215	197	258	27	87	107	278	172
211 - 220	234	15	38	223	296	71	152	188	119	59
221 - 230	204	248	134	83	178	284	158	2	33	100
231 - 240	262	214	235	274	23	65	291	121	199	44
241 - 250	171	146	90	10	246	132	56	108	222	163
251 - 260	74	255	181	211	30	277	194	293	93	149
261 - 270	116	80	266	7	53	238	37	137	175	231
271 - 280	67	202	14	160	288	112	259	41	86	218
281 - 290	124	185	19	155	281	243	97	49	129	226
291 - 300	26	270	168	62	190	76	251	104	207	142

TABLE II
 PUNCTURING POSITIONS FOR INNER CODE SYSTEMATIC BITS AND FIX PUNCTURING PATTERN $P_{o,1}$.

Index	Puncturing position									
1 - 10	101	1	193	285	341	49	145	241	369	313
11 - 20	73	169	217	25	265	121	385	325	85	357
21 - 30	297	181	229	37	133	253	13	61	157	205
31 - 40	108	276	345	389	309	89	373	329	196	40
41 - 50	148	244	8	64	124	220	172	292	260	360
51 - 60	96	20	396	281	184	136	232	52	333	76
61 - 70	160	208	112	305	257	377	349	33	317	80
71 - 80	268	392	176	128	212	45	353	152	236	300
81 - 90	105	16	201	68	365	272	140	5	321	225
91 - 100	92	165	29	288	380	188	336	249	274	48

TABLE III
 PUNCTURING POSITIONS FOR INNER CODE SYSTEMATIC BITS AND FIX PUNCTURING PATTERN $P_{o,2}$.

Index	Puncturing position									
1 - 10	1	398	10	272	105	176	338	226	58	138
11 - 20	305	369	35	203	83	251	154	320	120	290
21 - 30	352	386	16	209	64	232	170	41	266	99
31 - 40	184	0	344	299	146	89	257	376	128	314
41 - 50	216	48	360	162	112	282	24	192	240	72
51 - 60	330	392	136	280	26	194	74	242	328	50
61 - 70	218	378	114	160	306	354	264	90	18	186
71 - 80	144	370	288	235	57	337	106	8	211	168
81 - 90	385	322	122	258	66	296	42	152	362	248
91 - 100	200	96	312	32	130	178	346	274	224	80

TABLE IV
 PUNCTURING POSITIONS FOR INNER CODE SYSTEMATIC BITS CORRESPONDING TO OUTER CODE PARITY BITS AND FIX
 PUNCTURING PATTERN $P_{o,1}$.

Index	Puncturing position									
1 - 10	1	397	117	333	201	273	57	157	237	365
11 - 20	25	301	89	177	137	253	217	9	381	73
21 - 30	317	349	41	105	285	189	145	229	261	169
31 - 40	125	393	53	329	85	361	21	297	205	101
41 - 50	377	37	313	69	345	249	5	277	161	221
51 - 60	185	121	141	289	385	233	65	337	29	93
61 - 70	257	173	353	213	305	13	109	153	369	321
71 - 80	45	193	281	245	129	81	389	197	49	325
81 - 90	269	17	149	241	373	97	181	77	309	133
91 - 100	225	33	341	357	209	61	293	113	265	165

TABLE V

PARAMETERS OF THE RATE $R_{\text{SCCC}} = 2/3$ CODE WITH INTERLEAVER LENGTH N AND THE FIRST FIX PUNCTURING PATTERN $P_{o,1}$

ρ_p	$h_m^{(3)}$	$d^{o''} (d_f^{o'})$	$h(\alpha_M)$	h_m	N_{h_m}	Markers
20/300	0	3	3	3	3.60E-01	□
40/300	0	2	2	2	4.81E-03	+
60/300	0	2	2	2	7.12E-03	×
80/300	0	2	2	2	5.28E-03	△
100/300	0	1	1	1	1.40E-04	○

TABLE VI
PARAMETERS OF THE RATE $R_{\text{SCCC}} = 2/3$ CODE WITH INTERLEAVER LENGTH N AND THE SECOND FIX PUNCTURING
PATTERN $P_{o,2}$

ρ_p	$d_{f,\text{eff}}^2$	$d_f^{o''} (d_f^o)$	$h(\alpha_M)$	h_m	N_{h_m}	Markers
20/300	0	3	3	3	3.32E-01	□
40/300	0	2	2	2	5.24E-03	+
60/300	0	2	2	2	4.12E-03	×
80/300	0	2	2	2	1.98E-03	△
100/300	0	2	2	2	8.47E-04	○